

Horizontally Oriented Ice Crystals Observed with the Combination of Zenith and 15-degree off-Zenith pointing Polarization Lidar over Beijing (116.3°E 40.0°N), China

Zhaolong Wu^{(a)(b)}, Chengcai Li^(a), Yun He^{(b)(c)}, Holger Baars^(b), Patric Seifert^(b)

(a) School of Physics, Peking University, Beijing 100871, China

(b) Leibniz Institute for Tropospheric Research, Leipzig 04318, Germany

(c) School of Electronic Information, Wuhan University, Wuhan 430072, China
wuzhaolong@stu.pku.edu.cn

Abstract: We studied the horizontally oriented ice crystals (HOIC) with the combinational observations of a zenith-pointing and a slant-pointing (with a zenith angle of 15 degrees) polarization lidar in Beijing in 2022. The HOICs account for approximately 7.3 % of total ice-containing clouds. These results have the potential to enhance the parameterization scheme in climate models for this unique form of ice crystals.

1. Introduction

It has been recognized that under some specific conditions (Reynolds number between 1 and 100)[1] falling ice crystals in the atmosphere can become horizontally orientated. Horizontally oriented ice crystals (HOIC) possess the capability to reflect 40% more shortwave radiation into space compared to randomly oriented ice crystals[2], thereby significantly influencing the radiation balance. Despite its importance, limited knowledge exists regarding HOIC.

HOIC causes mirror-like specular reflection on the observations of zenith-pointing lidar, which is however not shown on that of slant-pointing lidar, i.e. very strong backscatter and near-zero depolarization for zenith-pointing lidar but relatively weaker backscatter and higher depolarization for slant-pointing lidar. This characteristic is beneficial to distinguishing the HOICs from other ice particles[1,3].

For the first time, the simultaneous observations using ground-based zenith and slant-pointing polarization lidars along with cloud radar, were conducted to study the HOIC in Beijing, China over 354 days in 2022.

2. Data

Two 532-nm polarization lidars were continuously running at Peking University (PKU). One zenith-pointing and one with an off-zenith angle of 15° (slanted pointing). The zenith-pointing lidar is a Micro Pulse Lidar manufactured by Sigma Space Corporation, while the slant-pointing lidar is produced by

AVORS Tech. The distance between the two lidars is about 5 meters (see Figure 1). Additionally, a Ka-band (33.44 GHz) zenith-pointing cloud radar was deployed to investigate the characteristics of HOIC[4]. ECMWF ERA5 reanalysis from the grid point of PKU (116.3°E 40.0°N) was used to provide the meteorological parameters, i.e., the temperature, wind, and specific humidity over ice.

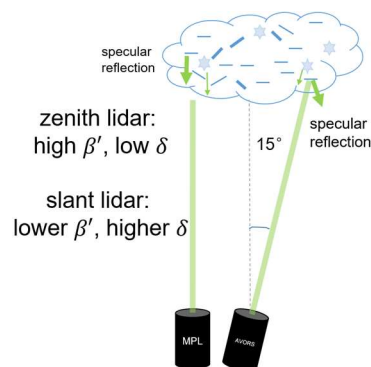


Figure 1. Schematic figure of the two lidars

3. Methods

PollyNet's method[5] was utilized for lidar calibration and subsequent derivation of the attenuated backscatter (β'). Subsequently, the lidar, radar, and ERA5 datasets were interpolated to uniform 15 m vertical grids and averaged to achieve a temporal resolution of 5 minutes. An advanced value distribution equalization method[6] was then applied to identify cloud pixels from the lidar attenuated backscatter coefficient signal. The overlap of cloud detection results from the two different lidars was analyzed to identify the relevant

cloud pixels. These intersecting cloud pixels, observed by both lidars, underwent cloud categorization using a specialized algorithm (Figure 2) to differentiate between different cloud phases.

Initially, we utilized the temperature of homogeneous nucleation (-38°C) to distinguish ice phase, followed by using the volume depolarization (0.1 and 0.3) to identify ice-containing cloud pixels at temperatures between 0 and -38°C . Then we used the zenith-to-slant ratio of the attenuated backscatter (threshold > 2) and the volume depolarization ratio (threshold < 0.6) as stringent criteria to exclusively capture the most representative signals of HOIC. On the contrary, ice pixels that do not meet the threshold are considered randomly oriented ice crystals.

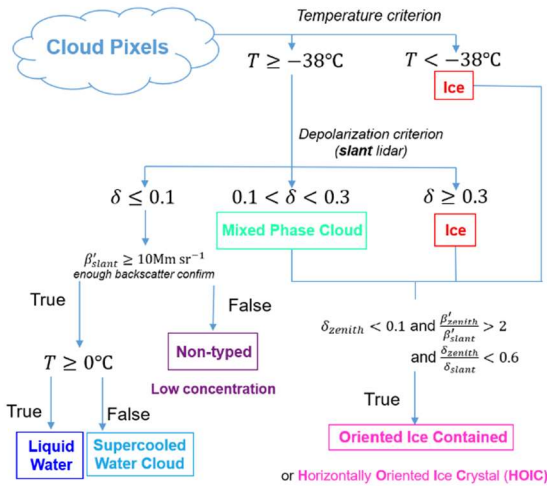


Figure 2. The algorithm for distinguishing the HOICs.

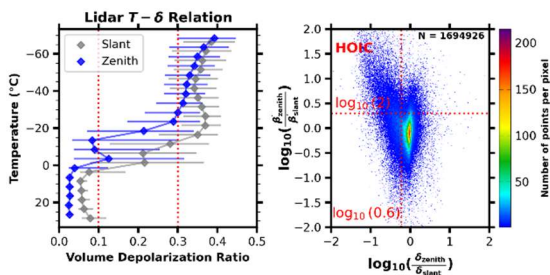


Figure 3. The criteria for distinguishing the HOICs (red dashed lines).

The criteria used to select a typical HOIC pixel are shown in Figure 3. The left panel is the median volume depolarization ratio as a function of temperature for each temperature bin within all detected cloud layers. Horizontal bars indicate the interquartile range (IQR). Zenith lidar shows much lower depolarization

than slant lidar between -20°C and 0°C . It probably is contaminated by HOIC. The right panel is the ratio of attenuated backscatter and depolarization ratio scatter plot on all cloud pixels detected. The left-top region indicates HOICs.

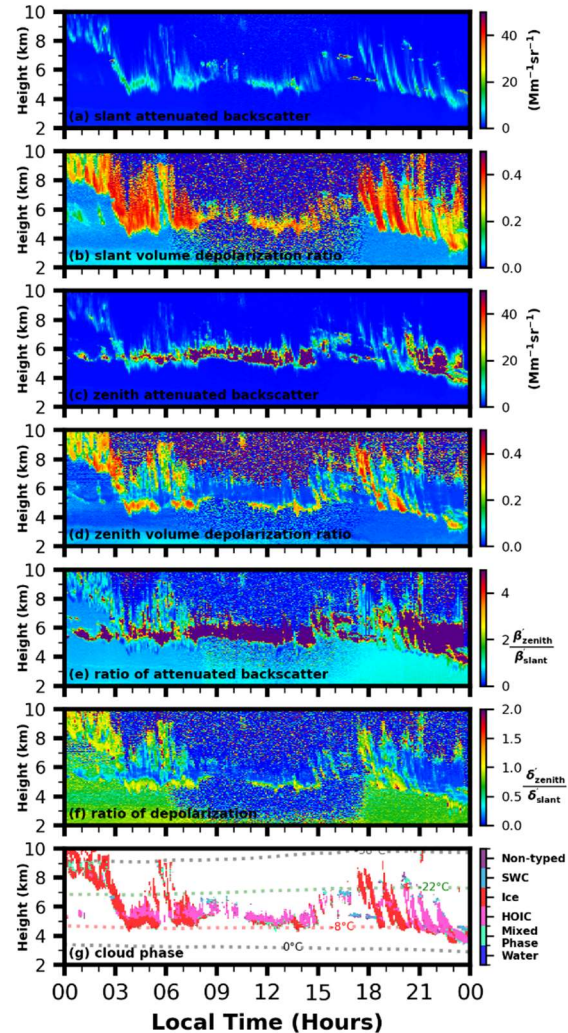


Figure 4. Lidar observations on Oct. 13, 2022.

4. Case study on 13th October

On 13th October, strong specular reflections were observed with the zenith-pointing lidar for almost the whole day, see Fig. 4. High backscatter and low depolarization ratio in zenith lidar observation and much lower backscatter and higher depolarization in slant lidar observation indicated the presence of HOICs. The HOIC flag by our algorithm is denoted in pink in Figure 4g.

This HOIC event existed for nearly the whole day. It is worth noting that some high depolarization ratio regions for zenith lidar

observation were observed below the strong specular reflection region.

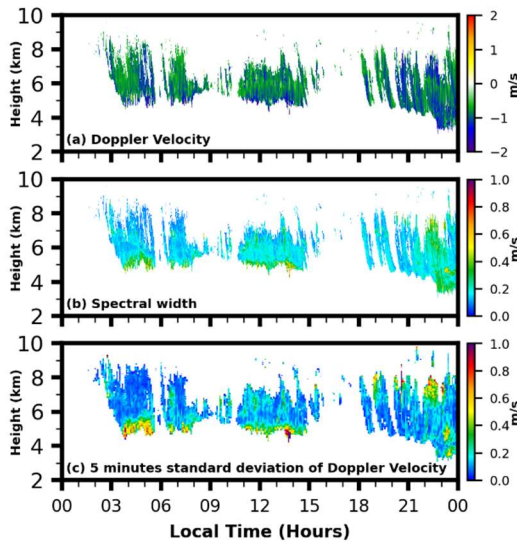


Figure 5 Zenith pointing cloud radar observations on Oct. 13, 2022.

The cloud radar observations (Fig. 5) show that the Doppler velocity changes significantly with time at the cloud base of such a high depolarization ratio region (compare Figures 5a and 4d). The high depolarization ratio region of the zenith lidar observation coincides also with a relatively higher spectral width of Doppler velocity (Fig. 5b). The standard deviation of Doppler velocity (Figure 5c) was computed to reflect the turbulent kinetic energy dissipation rate[7]. The high depolarization ratio region above the cloud base in the zenith lidar observation has a higher standard deviation of Doppler velocity, suggesting the strong turbulence caused by the latent heat released due to the evaporation of ice crystals near the cloud base.

5. Statistical Results

During 354 observation days in 2022, we collected 7930 hours of lidar data. There were 107700 pixels with HOICs observed, occupying 6.3% of all the clouds and 7.3% of the ice-containing clouds (see Figure 6). The ratio of HOIC to HOIC plus randomly oriented ice was 8.4%, which was slightly higher than 6% observed with CALIPSO [2].

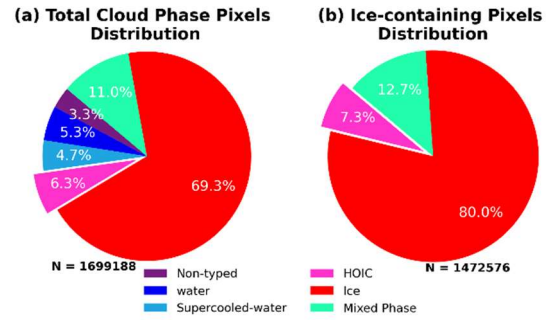


Figure 6 Statistics on cloud phase categorization for the entire year 2022

In general, the formation temperature of plate ice crystals, the main component of HOICs, is approximately -8 to -22°C according to laboratory research[8]. However, HOICs were still observed in this study at extremely low temperatures of $<-50^{\circ}\text{C}$. The statistical results (see Fig. 7) in 2022 showed that the median temperature in the presence of HOICs was -14.6°C , warmer than the temperature of -34.0°C associated with randomly oriented ice crystals. Furthermore, the median horizontal wind speed in the presence of HOICs (16.9 m/s) was lower than that associated with randomly oriented ice crystals (25.6 m/s). Additionally, the median altitude of HOICs (5.7 km) was lower than that of randomly oriented ice crystals (7.7 km). However, no difference in the relative humidity over ice was observed between the two types of ice crystals.

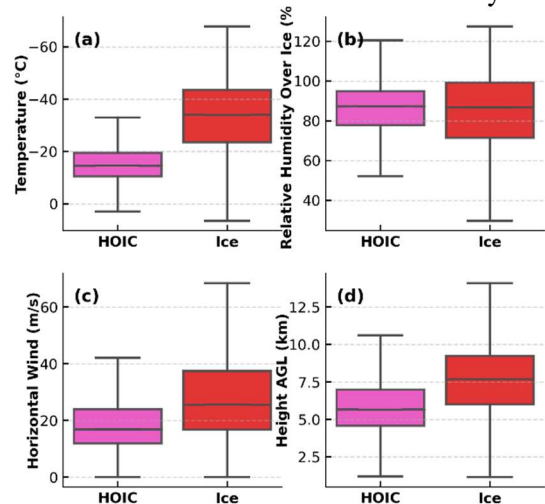


Figure 7 Comparison of conditions for HOICs and randomly oriented ice crystals in 2022. Boxes include the 25th to 75th percentiles and whiskers extend to the 10th and 90th percentiles.

6. Discussion and conclusion

Horizontally oriented ice crystals were observed over Beijing by the synergy of zenith and 15-degree off-zenith pointing polarization lidar and vertically pointing cloud radar in 2022. The fraction of HOIC in ice-containing cloud pixels was 7.3 %, with a median temperature of -14.6°C accompanied. These new results could contribute to new parameterization schemes for the weather and climate models. However, more detailed investigations are needed in the future. HOICs drop down with several flutter angles; thus, the relationship between turbulent kinetic energy dissipation and the flutter angle needs to be investigated quantitatively. Some model data could help on this topic. The relationship between the strength of turbulence and evaporation and its effect on ice orientation needs more careful comparison.

References

- [1] He Y, Liu F, Yin Z, et al, “Horizontally oriented ice crystals observed by the synergy of zenith- and slant-pointed polarization lidar over Wuhan (30.5°N, 114.4°E), China,” *J Quant Spectrosc Radiat Transf* **268**, 107626 (2021)
- [2] Noel V and Chepfer H, “A global view of horizontally oriented crystals in ice clouds from Cloud-Aerosol Lidar and Infrared Pathfinder Satellite Observation (CALIPSO),” **115**, 0–23 (2010)
- [3] Seifert P, “Dust-related ice formation in the troposphere: A statistical analysis based on 11 years of lidar observations of aerosols and clouds over Leipzig,” (2011)
- [4] Wang N, Zhang K, Shen X, et al, “Dual-field-of-view high-spectral-resolution lidar: Simultaneous profiling of aerosol and water cloud to study aerosol-cloud interaction,” *Proc Natl Acad Sci U S A* **119**, e2110756119 (2022)
- [5] Baars H, Kanitz T, Engelmann R, et al, “An overview of the first decade of PollyNET: An emerging network of automated Raman-polarization lidars for continuous aerosol profiling,” *Atmos Chem Phys* **16**, 5111–37 (2016)
- [6] Zhao C, Wang Y, Wang Q, et al, “A new cloud and aerosol layer detection method based on micropulse lidar measurements,” **119**, 6788–802 (2014)
- [7] O’connor E J, Illingworth A J, Brooks I M, et al, “A Method for Estimating the Turbulent Kinetic Energy Dissipation Rate from a Vertically Pointing Doppler Lidar, and Independent Evaluation from Balloon-Borne In Situ Measurements,” *J Atmos Ocean Technol* **27**, 1652–64 (2010)
- [8] Libbrecht K G, “The physics of snow crystals,” **68**, 855 (2005)